Neuron
Article

Neuregulin-1/ErbB Signaling Serves Distinct Functions in Myelination of the Peripheral and Central Nervous System

Bastian G. Brinkmann,[1,8] Amit Agarwal,[1,8] Michael W. Sereda,[1,2] Alistair N. Garratt,[3] Thomas Müller,[3] Hagen Wende,[3] Ruth M. Stassart,[1] Schanila Nawaz,[1] Christian Humml,[1] Viktorija Velanac,[1] Konstantin Radyushkin,[4] Sandra Goebbels,[1] Tobias M. Fischer,[1] Robin J. Franklin,[5] Cary Lai,[6] Hannelore Ehrenreich,[4] Carmen Birchmeier,[3] Markus H. Schwab,[1,*] and Klaus Armin Nave[1,7,*]

[1]Department of Neurogenetics, Max Planck Institute of Experimental Medicine, Goettingen 37075, Germany
[2]Departments of Neurology and Clinical Neurophysiology, University of Goettingen 37075, Germany
[3]Max Delbrueck Center for Molecular Medicine, Berlin 13092, Germany
[4]Division of Clinical Neuroscience, Max Planck Institute of Experimental Medicine, Goettingen 37075, Germany
[5]Department of Veterinary Medicine, Cambridge Center for Brain Repair, University of Cambridge, Cambridge CB3 0ES, UK
[6]Molecular and Integrative Neurosciences Department, The Scripps Research Institute, La Jolla, CA 92037, USA
[7]Hertie Institute for Multiple Sclerosis Research, Goettingen 37073, Germany
[8]These authors contributed equally to this work
*Correspondence: schwab@em.mpg.de (M.H.S.), nave@em.mpg.de (K.A.N.)
DOI 10.1016/j.neuron.2008.06.028

SUMMARY

Understanding the control of myelin formation by oligodendrocytes is essential for treating demyelinating diseases. Neuregulin-1 (NRG1) type III, an EGF-like growth factor, is essential for myelination in the PNS. It is thus thought that NRG1/ErbB signaling also regulates CNS myelination, a view suggested by in vitro studies and the overexpression of dominant-negative ErbB receptors. To directly test this hypothesis, we generated a series of conditional null mutants that completely lack NRG1 beginning at different stages of neural development. Unexpectedly, these mice assemble normal amounts of myelin. In addition, double mutants lacking oligodendroglial ErbB3 and ErbB4 become myelinated in the absence of any stimulation by neuregulins. In contrast, a significant hypermyelination is achieved by transgenic overexpression of NRG1 type I or NRG1 type III. Thus, NRG1/ErbB signaling is markedly different between Schwann cells and oligodendrocytes that have evolved an NRG/ErbB-independent mechanism of myelination control.

INTRODUCTION

The neuronal growth factor Neuregulin-1 (NRG1) comprises a family of more than 15 transmembrane and secreted proteins, derived from one of the largest mammalian genes. All NRG1 subtypes share an epidermal growth factor (EGF)-like signaling domain and can be classified into subgroups through their different amino termini (Falls, 2003). NRG1 isoforms type I and type II have N-terminal Ig-like domains and, following proteolytic cleavage, can be shed and released as soluble proteins from the neuronal cell surface. NRG1 type III is defined by a cysteine-rich domain (CRD), has two transmembrane domains, and is tightly associated with axonal membranes (Esper et al., 2006; Nave and Salzer, 2006).

The best understood function of NRG1 is the control of myelination in the peripheral nervous system (PNS), where NRG1 is essential for glial and neuronal survival, the proliferation of Schwann cells, and their terminal differentiation (Garratt et al., 2000a; Nave and Salzer, 2006). In development, a threshold level of axonal Nrg1 type III is required to induce myelination by Schwann cells in vitro and in vivo (Taveggia et al., 2005) (M.H.S. et al., unpublished data). Both Schwann cell expansion and myelination require glial ErbB2 receptors (Garratt et al., 2000b). Subsequently, the amount of NRG1 type III expressed on myelinated axons determines myelin sheath thickness (Michailov et al., 2004). At this stage, proteolytic processing may be required to fully activate NRG1 type III (Hu et al., 2006; Sagane et al., 2005; Willem et al., 2006).

In the central nervous system (CNS), NRG1/ErbB signaling has been implicated in a broad range of roles, including neuronal migration, axonal pathfinding, and synaptic function (Flames et al., 2004; Lopez-Bendito et al., 2006; Mei and Xiong, 2008). NRG1 signaling also affects oligodendrocyte specification, differentiation, myelination, and survival, at least in vitro (Calaora et al., 2001; Canoll et al., 1996, 1999; Flores et al., 2000; Vartanian et al., 1997).

The embryonic lethality of null mutations has hampered the in vivo analysis of *Nrg1* and *ErbB* in the nervous system (Adlkofer and Lai, 2000; Garratt et al., 2000b). Nevertheless, several ex vivo studies supported a possible role of both genes in oligodendrocyte differentiation and myelination (Fernandez et al., 2000; Park et al., 2001; Sussman et al., 2005; Vartanian et al., 1999). Moreover, heterozygous NRG1 type III mutants were reported to be hypomyelinated (Taveggia et al., 2008), and transgenic mice overexpressing dominant-negative ErbB receptors in oligodendrocytes (Kim et al., 2003; Roy et al., 2007) suggested a critical function of NRG1/ErbB signaling in CNS myelination.

Independently, the identification of *Nrg1* as a susceptibility gene in human schizophrenia (Law et al., 2006; Stefansson et al., 2002) has renewed interest in the contribution of NRG1/ErbB signaling to mammalian brain development, including CNS myelination, as some patients with schizophrenia show white matter abnormalities (Corfas et al., 2004). In addition, the demonstration of a myelin-promoting function of NRG1 in vivo could aid the development of a therapeutic strategy for demyelinating diseases such as multiple sclerosis.

To determine the consequences of altered NRG1/ErbB signaling on brain development, and specifically on the myelination of CNS fiber tracts, we generated and analyzed a large battery of mice with reduced *Nrg1* gene dosage, neuronal NRG1 overexpression, various conditional *Nrg1 null* mutations (defined by Cre recombination at different stages of development), and mice lacking oligodendroglial ErbB3 and ErbB4 receptors. Collectively, these data demonstrate that axonal NRG1/ErbB signaling plays a fundamentally different role in central and peripheral myelination.

RESULTS

Many CNS axons are first myelinated by oligodendrocytes and then by Schwann cells as they exit the spinal cord. Schwann cells can also invade the demyelinated CNS and ensheath central axons. These observations suggest that the axonal signals controlling myelin formation are conserved in the central and peripheral nervous systems (Colello and Pott, 1997; Duncan and Hoffman, 1997). Since heterozygous *Nrg1 null* (affecting all isoforms) mice exhibit a significant hypomyelination of axons in the PNS (Michailov et al., 2004; Taveggia et al., 2005), we anticipated a corresponding hypomyelination also in CNS white matter tracts. Surprisingly, analysis of the optic nerve, corpus callosum, and spinal cord of adult *Nrg1 null* heterozygous (+/−) mice revealed no such reduction of myelin sheath thickness by electron microscopy (Figure S1A) and subsequent calculation of g ratios when plotted as a function of the axonal caliber (Figure S1B). Also, mice heterozygous for only the NRG1 type III isoform (Wolpowitz et al., 2000) exhibited normal myelin thickness in the corpus callosum (Figures S1C and S1D). Both findings are at variance with a recent report (Taveggia et al., 2008). Supportive evidence for our findings (in addition to the data below) is that heterozygous mice of either mutant allele (*Nrg1 null* or *type III* specific) express the same steady-state level of NRG1 protein in brain (Figure S1E) and spinal cord (data not shown) when compared to wild-type controls.

Myelination in the Absence of NRG1

Conventional *Nrg1* null (−/−) mice die at embryonic day (E) 10.5, prior to the generation of oligodendrocytes. We therefore generated conditional *null* mutants to analyze possible defects of postnatal CNS myelination. Mice carrying two "floxed" *Nrg1* alleles readily recombine exons 7–9 (essential for the EGF-like signaling function) upon Cre expression in vivo (Li et al., 2002).

By crossbreeding floxed *Nrg1* to CamKII-Cre mice (Minichiello et al., 1999), we obtained mutants lacking NRG1 in virtually all projection neurons of the forebrain (Figures S2A and S2B) due to Cre recombination at around postnatal day (P) 5, i.e., after oligodendrocyte specification but prior to subcortical myelination. Surprisingly, these mutants revealed no obvious developmental abnormalities of the cortex, hippocampus, or the subcortical white matter and showed no demyelination at older age (Figures S2C and S2D). Although some myelination may have occurred prior to the complete loss of NRG1 protein, we conclude that axonal NRG1 is not required to maintain CNS myelin throughout adult life.

In order to address the developmental role of NRG1, we generated mutants using Cre recombination during the embryonic period. By crossbreeding floxed *Nrg1* with *NEX-Cre* mice (Goebbels et al., 2006), we disrupted NRG1 expression in newborn projection neurons of the cortex beginning at E12, including virtually all neurons that extend axons into the corpus callosum (Figure S2E).

Surprisingly, *NEX-Cre*Nrg1*$^{flox/flox}$ mutants ("NC*F/F") were fully viable and indistinguishable in the cage from wild-type, floxed ("F/F"), or *NEX-Cre*Nrg1*$^{flox/+}$ controls. By morphological and immunohistochemical criteria, the cortex and hippocampus appeared normal (Figure 1A and data not shown). Efficient Cre-mediated recombination was demonstrated by PCR analysis of brain genomic DNA at 3 months of age (data not shown). Quantitative RT-PCR (data not shown) and western blotting (Figure 1B) confirmed the reduction of NRG1, with residual expression most likely derived from glia (Esper et al., 2006). The subcortical white matter with callosal axons from the overlying cortical projection neurons was well developed (Figure 1A), and myelin proteins were expressed at wild-type levels (Figure 1C). We observed that myelinated fibers in the gray matter were normal in appearance when immunostained for 2′ 3′-cyclic nucleotide phosphodiesterase (CNP) (Figures 1D and 1E) or MBP (data not shown).

Using electron microscopy, myelin in the corpus callosum (Figure 2A) and the spinal cord (data not shown) of 11-week-old mice exhibited an intact ultrastructure. There were no obvious differences in myelin sheath thickness or axonal size distribution (Figure 2B). Also, at 2 years of age, there were no signs of hypomyelination, demyelination, or axonal degeneration in these mice, as demonstrated by electron microscopy of the corpus callosum (Figures 2C and 2D).

To address a potential myelination delay in the absence of NRG1, we immunostained MBP at postnatal day (P) 10. Confocal microscopy revealed unaltered numbers of MBP+ myelin profiles in the ventral corpus callosum of NC*FF mutants when compared to controls (Figures 2E and 2F), demonstrating also that timely myelination does not depend on NRG1.

Recently, hypomyelination in the CNS was reported in mice lacking the expression of BACE1, a protease required for NRG1 processing (Hu et al., 2006; Willem et al., 2006). This suggests that widespread BACE1 activity could provide a "paracrine" source of NRG1 originating from astrocytes (Esper et al., 2006) that are genetically "wild-type" in *NEX-Cre*NRG1*$^{flox/flox}$ mice. To inactivate possible astroglial and oligodendroglial sources of NRG1 in the developing CNS, we generated conditional *Emx-Cre*Nrg1*$^{flox/flox}$ null mutants that recombine efficiently in multipotential progenitors of the embryonic forebrain (Gorski et al., 2002). When analyzed at adult age (4 months), these mice were fully myelinated (data not shown) without morphological or biochemical differences between wild-type and mutants (Figures S3A and

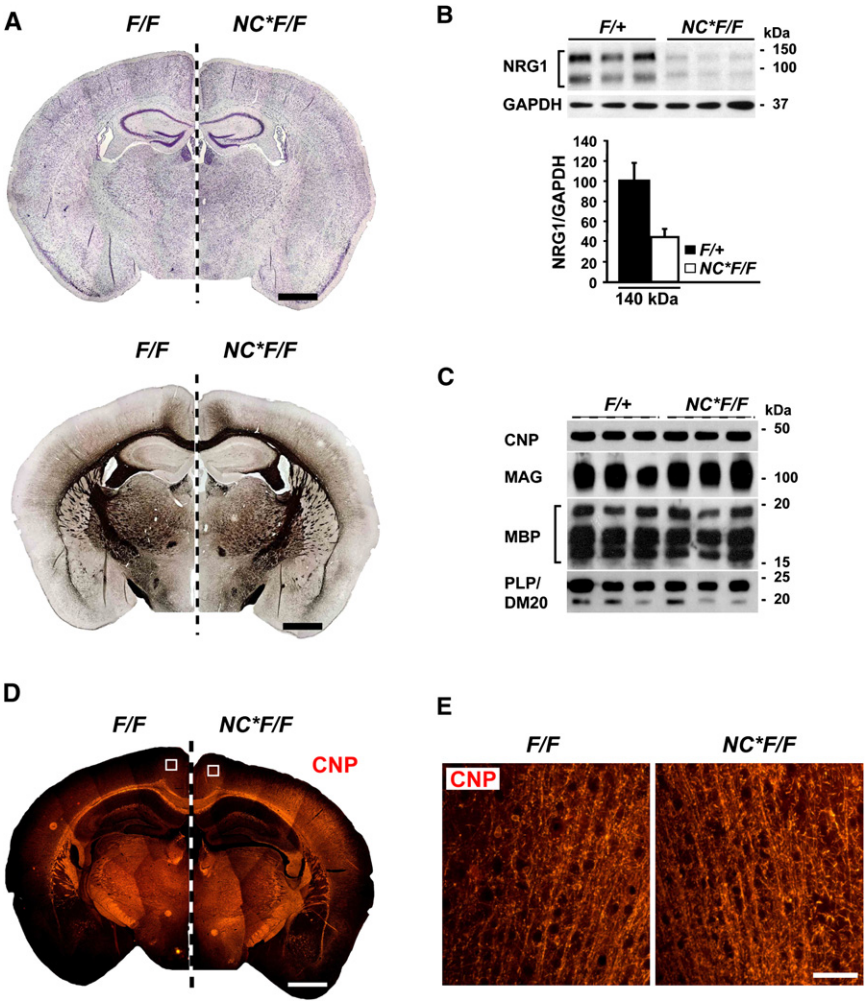

Figure 1. Myelination in *NEX-Cre*Nrg1*$^{flox/flox}$ Mice following Embryonic Recombination

(A) Neocortical development (Nissl staining) and subcortical myelination (Gallyas silver impregnation) appear normal in mutant mice (*NC*F/F*) compared to controls (*F/F*). Depicted are mirror images of coronal paraffin sections (7 μm) obtained at age 3 months. Scale bars, 1 mm.

(B) (Top) Western blot of protein lysates revealing a loss of NRG1 in the neocortex of *NC*F/F* mutants compared to controls (F/+) at 3 months of age. (Bottom) Densitometric quantification reveals an ~60% reduction of "full-length" NRG1 type III (~140 kDa) in *NC*F/F* mutants compared to controls (*F*/+). Peak intensities (±SEM) were normalized to GAPDH.

(C) Semiquantitative comparison of myelination by western blotting myelin-specific proteins from neocortical protein lysates of mutant mice (*NC*F/F*; age 3 months) and littermate controls (*F*/+). Steady-state levels of CNP, MAG, MBP, and PLP/DM20 are normal.

(D and E) Myelinated tracts in neocortex and corpus callosum of mutants (*NC*F/F*), as visualized by immunostaining for CNP. Shown are coronal paraffin sections (7 μm) of 3-month-old brains from mutants (*NC*F/F*; right hemisphere) and control mice (*F/F*; left hemisphere). Scale bar, 1 mm. Enlargements in (E) reveal individual fibers in cortical layers II/III (boxed in upper panels). Scale bar, 50 μm.

S3B), except for the nearly complete absence of NRG1 in brain lysates (data not shown).

To completely abolish NRG1 expression in the developing CNS, we generated conditional mutants using *Nestin-Cre* mice (Tronche et al., 1999) (Figures S4A and S4B). *Nestin-Cre*Nrg1*$^{flox/flox}$ mutants died about 16 hr after birth, i.e., later than conventional *Nrg1 type III null* mutants (Wolpowitz et al., 2000) but most likely with a lethal PNS defect (see below and Figures S4C and S4D). When *Nestin-Cre* mutants were analyzed at birth, there was no detectable difference in brain morphology compared to controls (Figure 3A). Western blotting showed mutant brains to be almost completely NRG1 deficient (Figure 3B, top). Also, in spinal cord, NRG1 was dramatically reduced (Figure 3B, bottom). Quantitative RT-PCR confirmed the virtual absence of NRG1 in brain and a severe reduction in spinal cord, with residual protein expression most likely derived from the central branch of inefficiently recombined DRG neurons (Figure S4B). Spinal cord ventral roots, harboring the peripheral aspects of motoneuron axons, as well as intercostal nerves, almost completely lacked MBP and MPZ (P0) immunostaining, demonstrating a block of Schwann cell differentiation in *Nestin-Cre*Nrg1*$^{flox/flox}$ mutants (Figure 3C, middle and bottom panel). Accordingly, immunostaining of sciatic nerves derived from newborn *Nestin-Cre*Nrg1*$^{flox/flox}$ mice revealed a strong reduction in the number of MPZ-stained myelin profiles and Krox20-stained myelinating Schwann cells (Figures S4C and S4D).

Unexpectedly, the density of Olig2+ and MBP+ oligodendrocytes in the forebrain and spinal cord of these mice (Figure 3D and data not shown) did not obviously differ in mutants and controls (not quantified). Similarly, in the spinal cord, there was no difference in the density of MBP+ myelin profiles in *Nestin-Cre*Nrg1*$^{flox/flox}$ mice at birth (Figure 3C, upper panel). While these data do not rule out a function for NRG1 as a growth or survival factor in the oligodendrocyte lineage, myelinating glial cells clearly develop in the absence of NRG1 in vivo.

Since *Nestin-Cre*Nrg1*$^{flox/flox}$ mice died many days prior to myelin formation in the subcortical white matter, we also compared long-term cocultures of wild-type oligodendrocytes and cortical neurons, derived from embryonic wild-type or Nrg1 *null* mice. As expected, myelination of the NRG1-deficient CNS axons could be readily demonstrated by MBP immunostaining (Figure S5A) and was independently observed in mixed brain cultures derived solely from *Nestin-Cre*Nrg1*$^{flox/flox}$ mice (Figure S5B).

Myelination in the Absence of ErbB Signaling

The receptor tyrosine kinases ErbB2 and ErbB4 have been suggested to control CNS myelination in vivo (Vartanian et al., 1997), while ErbB3 is not required for oligodendrocytic differentiation

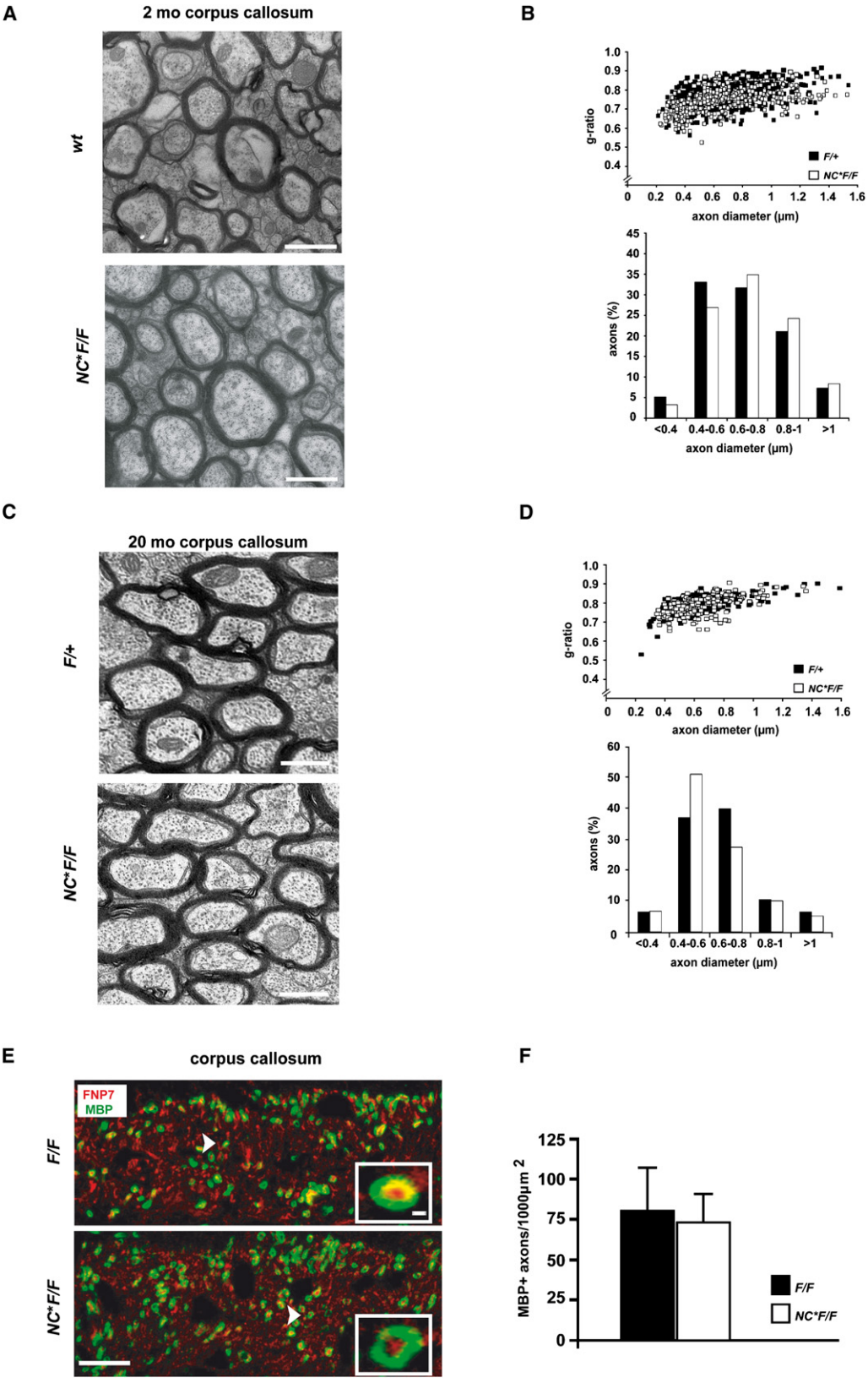
A
2 mo corpus callosum
wt
NC*F/F
B
g-ratio
axon diameter (μm)
F/+
NC*F/F
axons (%)
<0.4
0.4-0.6
0.6-0.8
0.8-1
>1
C
20 mo corpus callosum
F/+
NC*F/F
D
E
corpus callosum
FNP7
MBP
F/F
NC*F/F
F
MBP+ axons/1000μm 2

(Schmucker et al., 2003). We first studied myelination in mice that lacked ErbB4 but were rescued from embryonic lethality by means of an MHC-ErbB4 transgene expressed in the heart (Tidcombe et al., 2003). Myelination appeared normal in the CNS of these ErbB4 mutant mice, and there was no paucity of Olig2+ oligodendrocytes (data not shown). Examination by electron microscopy revealed that homozygous *ErbB4* null mutants had no dysmyelination phenotype (Figure 4A). When quantified in the corpus callosum, g ratios of myelinated axons in ErbB4 null mutant mice were the same as in controls (Figure 4B).

All neuregulins (NRG1, NRG2, NRG3) signal via ErbB2, ErbB3, and ErbB4 receptor homo/heterodimers. Since ErbB2 lacks ligand-binding activity, the absence of both ErbB4 and ErbB3 from oligodendrocytes should suffice to completely eliminate neuregulin signaling. We therefore generated a floxed allele of the *ErbB3* gene (T.M., H.W., and C.B., unpublished data) and crossed these conditional mutants to a conditional *null* mutant of the *ErbB4* gene (Golub et al., 2004). Efficient recombination of both genes in oligodendrocytes using CNP-Cre mice (Lappe-Siefke et al., 2003) was confirmed by PCR on genomic DNA derived from cortex and optic nerve (data not shown). As expected, we detected by quantitative real-time PCR a severe reduction in ErbB3 and ErbB4 expression in various CNS regions (including optic nerve; Figures S3C and S3D) with residual mRNA most likely derived from nonoligodendroglial cells.

*CNP-Cre*ErbB3*$^{flox/-}$ single mutants (harboring one copy of the conventional *erbB3 null* allele; Riethmacher et al., 1997) and CNP-*Cre*ErbB3*$^{flox/-}$**ErbB4*$^{flox/flox}$ double mutants developed to term. As expected, they displayed severe defects in PNS myelination (Figure 4C, bottom panel) and died in the second postnatal week. In striking contrast, electron microscopy of the optic nerve and corpus callosum (Figure 4C, upper and middle panel), g ratio measurements (Figure 4D, optic nerve only), and immunostaining for MBP (data not shown) clearly demonstrated that oligodendrocytes in ErbB3*ErbB4 double mutants (*CNP-Cre*ErbB3*$^{flox/-}$**ErbB4*$^{flox/flox}$) were capable of myelinating CNS axons without delay and at the same level as control mice (*ErbB3*$^{flox/+}$**ErbB4*$^{flox/+}$), at least up to postnatal day P11. Although we cannot rule out phenotypic differences at later stages, we conclude that neuregulin/ErbB signaling is dispensable for CNS myelination in vivo.

Myelination in Response to NRG1 Type I and Type III Overexpression

While myelination is independent of NRG1 in vivo, cells of the oligodendrocyte lineage clearly respond to the soluble growth factor in culture (Calaora et al., 2001; Fernandez et al., 2000; Flores et al., 2000; Kim et al., 2003; Vartanian et al., 1997, 1999). To determine what type of responsiveness oligodendrocytes show to axonal NRG1 in vivo, we analyzed mice that overexpress cDNAs encoding NRG1 type III (or NRG1 type I) under control of the neuronal Thy1.2 promoter (Michailov et al., 2004). All NRG1 overexpressing mice were viable, but those with higher transgene dosage exhibited ataxia that was most pronounced in homozygous mice and that precluded detailed behavioral testing (data not shown). The cause of these neurological abnormalities is unknown, but given the broad expression of NRG1 and ErbB receptors, it could be due to abnormal neuronal differentiation, synaptic function, myelination, muscle development, or any combination of these. By immunocytochemical analyses, the overexpression of NRG1 type I or NRG1 type III was widespread throughout the cortex in all lines tested (Figure S6A and data not shown). Expression analysis by quantitative RT-PCR (Figure S6B) and western blotting (Figure S6C) demonstrated that NRG1 steady-state levels were about 5-fold increased in adult heterozygous Thy1-Nrg1 type I and type III transgenic mice.

Although morphological effects were not dramatic, we found many "hypermyelinated" axons in the white matter regions analyzed. By electron microscopy, these axon-myelin units were regularly spaced, and hypermyelination was clearly the result of additional spiral wraps (Figure 5A). Unexpectedly, decreased g ratios were also observed in Nrg1 type I transgenic mice (Figure 5B), not only in type III transgenics (Figure 5C). This revealed an important difference between the CNS and PNS, where only the overexpression of axon-bound NRG1 type III induces hypermyelination (Michailov et al., 2004). It is conceivable that (shed) NRG1 type I acts by stimulating oligodendrocyte production prior to myelination and that an altered axon-glia ratio is the basis of hypermyelination. We therefore compared the density of CC1+ and CNP+ oligodendrocytes within the corpus callosum of type I transgenic and wild-type mice but found no significant differences (Figure S6D and data not shown).

Also axons within the cortex (layers II and III), which are generally of small caliber, showed a significant decrease of g ratios (Figures 6A and 6B). In Nrg1 type I transgenics, such a hypermyelination was only a feature of axons thinner than 0.4 μm (leading to a crossing of regression lines). Interestingly, in both transgenic lines, we noticed a 2-fold increase of myelinated fibers per cross-sectional area (upper cortical layers; white arrowheads in Figure 6C) when compared to controls (Figure 6D). However, there was no corresponding increase in the density of (CC1+) oligodendrocytes (Figure 6E).

Possible explanations for the 2-fold higher "myelin-to-oligodendrocyte" ratio in the cortex could be an increase of internodal

Figure 2. Myelination and Myelin Ultrastructure in the Absence of NRG1

(A) Electron microscopy reveals normally myelinated axons in the corpus callosum of mutant (*NC*F/F*) and control mice (wild-type and F/+) at 11 weeks of age.

(B) G ratio analysis and scatter blots derived from electron micrographs of the corpus callosum in mutant (*NC*F/F*) and control mice, aged 11 weeks (n = 7 per genotype). Quantitation of axon size distribution reveals no obvious difference between mutants (white bars) and controls (black bars).

(C) Also in aged mice (>18 months), electron microscopy of the corpus callosum demonstrates intact myelin profiles and the absence of neurodegeneration in mutant (*NC*F/F*) and control (F/+) mice. Scale bars, 1 μm.

(D) Quantitation (g ratios) of the data in (C) reveals no dys- or demyelination (n = 3 per genotype).

(E) Callosal myelination in the absence of NRG1 is not delayed (age P10). Confocal microscopy of coronal vibratome sections (100 μm) immunostained for axons derived from projection neurons (FNP7, red) and myelin (MBP, green) demonstrates widespread myelination in the ventral corpus callosum of mutant (*NC*FF*) and control (*F/F*) mice. Scale bar, 10 μm (inset, 250 nm).

(F) Quantitation of MBP data in (E) (n = 3 per genotype; ±SEM).

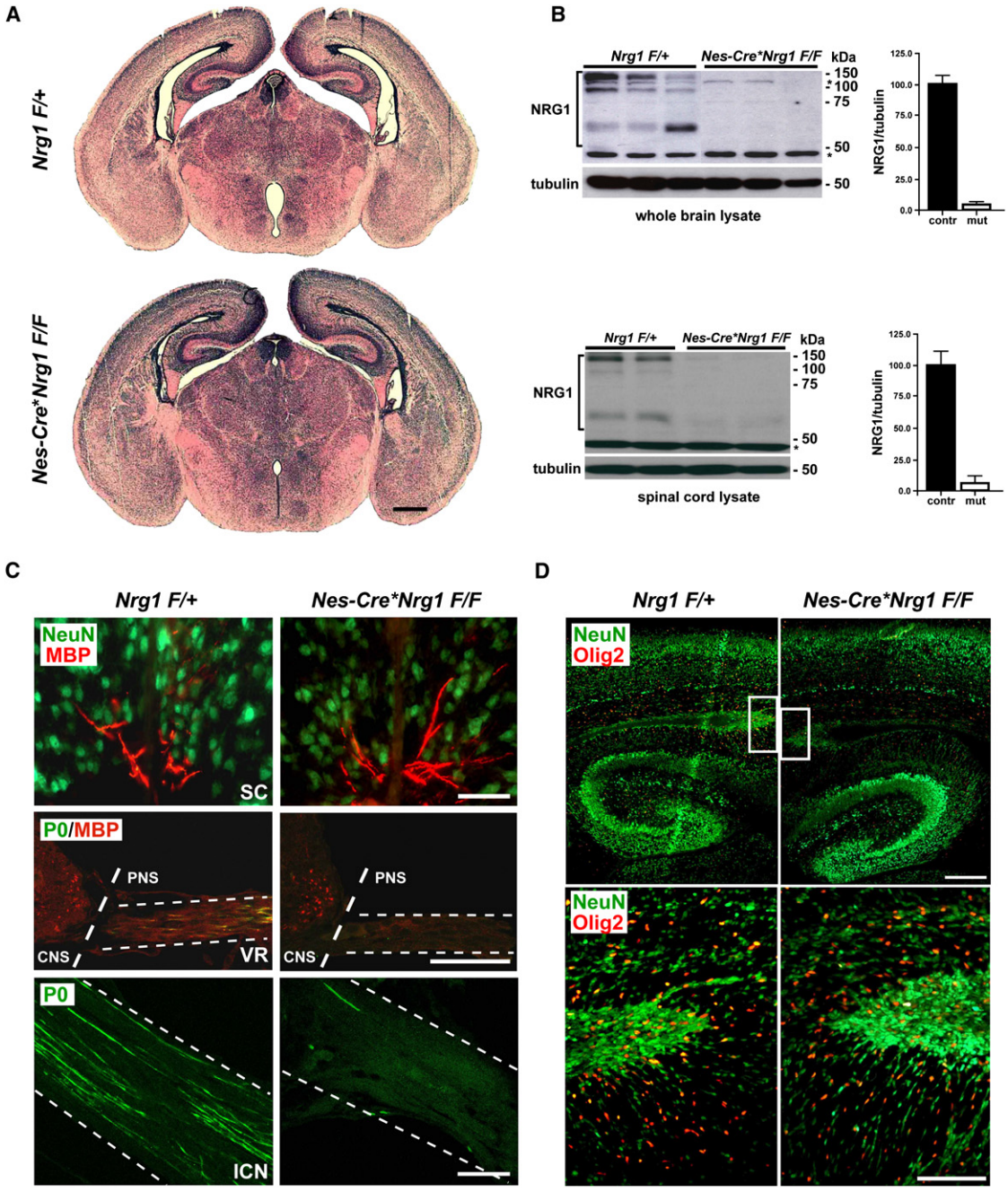

Figure 3. Oligodendrocytes Develop on Schedule in the Absence of NRG1

(A) Cortical and hippocampal development in *Nestin* (*Nes*)-*Cre***Nrg1F/F* mice that recombine in all neural precursor cells beginning at E8.5 is without obvious delay or morphological defect (see Figure S2A). Shown are H&E-stained frontal brain sections (7 μm, paraffin) of newborn controls (*Nrg1F/+*, top) and mutants (bottom). Scale bar, 500 μm.

(B) NRG1 is virtually absent in the CNS of newborn *Nes-Cre***Nrg1F/F* mutant mice. Western blot analysis of protein lysates prepared from brain (top panel) and spinal cord (lower panel), comparing three control mice (*Nrg1F/+*, left) and three conditional *null* mutants (*Nes-Cre***Nrg1F/F*, right). Densitometry of brain and spinal cord immunoblots revealed an ~95% reduction of NRG1 in mutants compared to controls. Mean intensities (±SEM) were normalized to α-tubulin. One brain (upper lane 3) was isolated 2 hr after natural death, showing some postmortem proteolysis. Molecular weights of marker proteins are indicated (asterisks denote unspecific bands; loading control, tubulin).

(C) Impaired peripheral but not central myelination. (Top) Immunostaining of the ventro-medial spinal cord from newborn mice reveals the normal density of MBP+ myelin profiles (in red) in NRG1-deficient (*Nes-Cre***Nrg1F/F*, right) and control mice (*Nrg1F/+*, left). Neurons are stained for Neu-N (in green). (Middle) Immunostaining of cross-sections at the thoracic level for MBP (in red) and myelin protein zero (P0; in green). Note the almost complete absence of MBP and P0 in the ventral roots (VR; also marked "PNS") of newborn *Nes-Cre***Nrg1F/F* mutants (right). In contrast, littermate *Nrg1F/+* controls (left) exhibit numerous myelinated

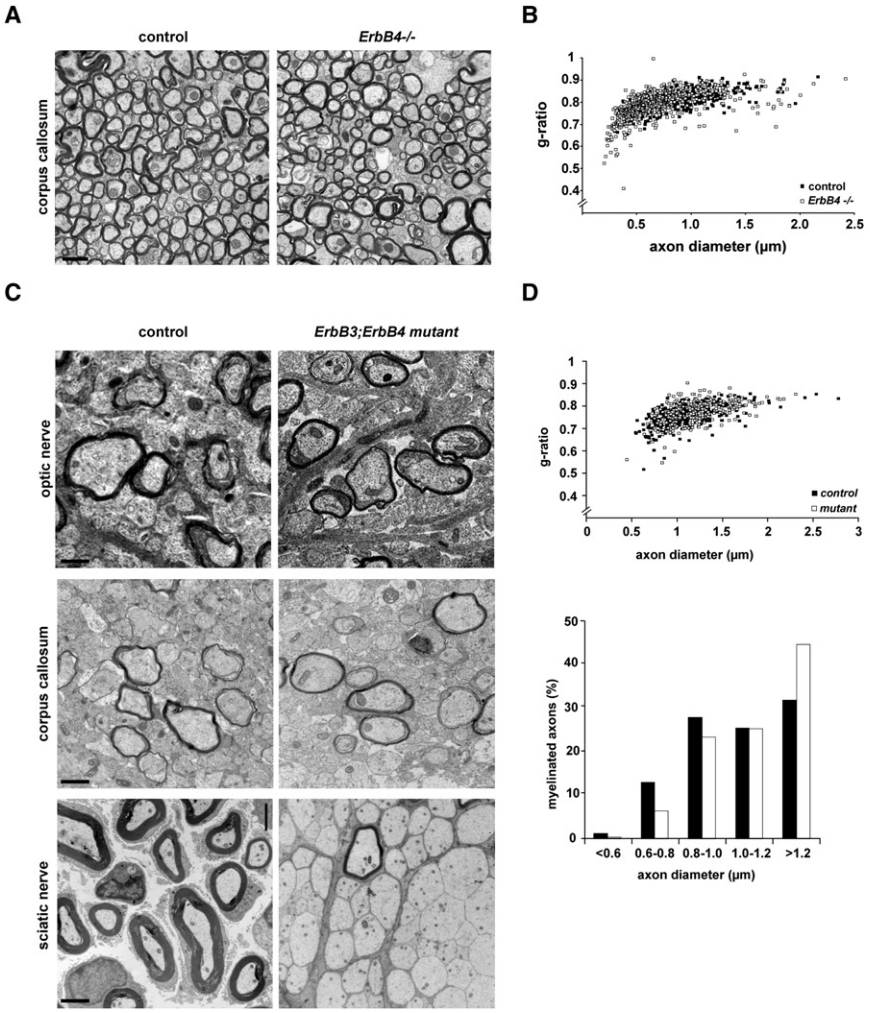

Figure 4. Myelination in the Absence of ErbB3 and ErbB4 Receptors

(A) Electron micrographs showing myelinated axons of the anterior corpus callosum in adult wild-type mice (labeled "control") and transgenically rescued ErbB4 single mutants (genotype *MHC-ErbB4*ErbB4*$^{-/-}$), labeled "ErbB4−/−." Scale bar, 2 μm.

(B) Quantitation of myelin sheath thickness in the corpus callosum by g ratio analysis of electron micrographs, comparing control mice (black circles, n = 3) and rescued *ErbB4*$^{-/-}$ mutants (n = 3, open circles). Scatter plot displays g ratios of individual fibers as a function of the respective axon diameter. Myelin sheath thickness is not significantly different.

(C) Electron micrographs of the optic nerve (top), corpus callosum (middle), and sciatic nerve (bottom) at age P11 from ErbB3*ErbB4 double mutants (right; genotype *Cnp-Cre*ErbB3F/-*ErbB4F/F*) and controls (genotype *ErbB3F/+*ErbB4F/+*). Axons in the optic nerve and corpus callosum of ErbB3*ErbB4 double mutants are normally myelinated, whereas myelination of the sciatic nerve is severely impaired. Scale bars, 1 μm (optic nerve, corpus callosum); 2 μm (sciatic nerve).

(D) Quantitation of myelin sheath thickness (g ratios) and axon size distribution for the optic nerve of ErbB3*ErbB4 double mutants and controls (age P11; n = 3 per genotype) reveals no significant difference between mutants (white circles and bars) and controls (black circles and bars).

length and/or a higher number of internodes (i.e., oligodendrocyte processes) in NRG1 overexpressing mice. Since an unbiased quantitation of internodal length is difficult within cortical sections, we performed confocal microscopy and three-dimensional cell tracing of selected, singly located (CNP-stained) oligodendrocytes in layers II and III of the cingulate and primary motor cortex (Figure 7A). In the absence of pathological signs, the average number of processes (Figure 7B), process branch points (Figure 7C), and process length including internodal myelin (Figure 7D) was not significantly altered in *Nrg1* mutants and NRG1 type III overexpressing mice. Only the average "territory" of these oligodendrocytes (Figure 7E) was significantly higher in transgenics (+50%), similar to the increased volume of the oligodendroglial somata (Figure 7F). Thus, cortical hypermyelination cannot be fully explained by a numerical increase of oligodendrocyte processes in the cortex of NRG1 type III overexpressing mice. Outside the cortex, we never found "ectopic" ensheathment of axons that normally remain unmyelinated (such as mossy fibers in the hippocampus), although in transgenic mice dentate gyrus granule cells expressed visibly more NRG1 (data not shown).

While myelination was not delayed even in the absence of NRG1 (Figures 2E and 2F), there was clear evidence for premature myelination in NRG1 type III overexpressing mice (Figure 8A). For example, *Nrg1* mRNA in retinal ganglion cells was further enhanced in early postnatal mice by expression of the Thy1-Nrg1 type III transgene (Figures 8B and 8C). In these developing optic nerves, we determined a 3-fold higher number of myelinated axons than in controls (day P6; Figure 8D), without a corresponding shift of oligodendrocyte numbers (Figure 8E). This demonstrates that NRG1 can initiate the myelination program in CNS development, a function normally provided by a distinct (yet unknown) axonal signaling system. We also conclude

(MBP+/P0+, merged) axons. Note the presence of MBP+ oligodendrocytes in the ventro-lateral spinal cord (marked "CNS") in both mutants and controls. (Bottom) Immunostaining of longitudinal sections of the intercostal nerve (ICN) reveals absence of P0-stained fibers (in green) in newborn *Nes-Cre*Nrg1F/F* mutants (right) when compared to littermate controls (left). Scale bars, 50 μm.

(D) Olig2+ oligodendrocytes (in red) are present at a normal density and with a similar distribution in the forebrain of newborn mutant mice (*Nes-Cre*Nrg1F/F*, right) compared to controls (*Nrg1F/+*, left). Boxed areas in upper panel are enlarged in lower panel. Neurons are stained for NeuN (in green). Scale bars, 200 μm (upper panel), 100 μm (lower panel).

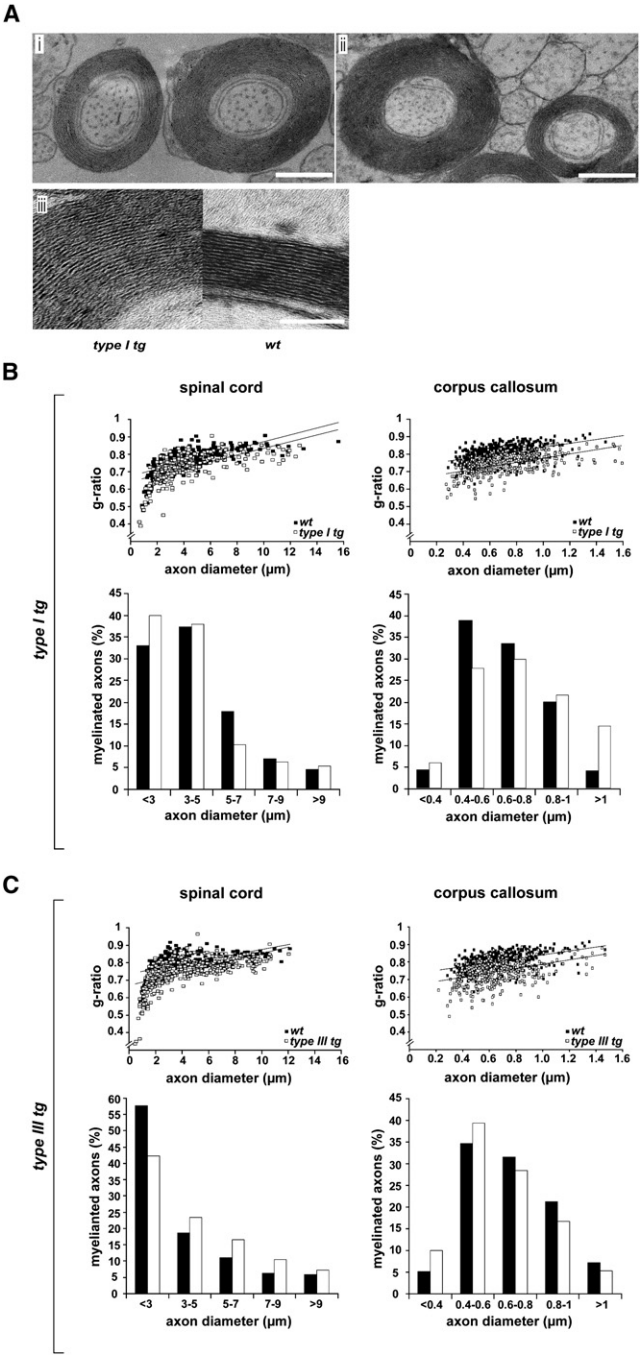

Figure 5. Transgenic Overexpression of NRG1 Type I or Type III Causes Hypermyelination

(A) Electron microscopy of hypermyelinated callosal axons in transgenic mice (age 4.5 months) overexpressing (Ai) NRG1 type I and (Aii) NRG1 type III under control of the neuronal Thy1.2 promoter. (Aiii) Ultrastructure of CNS myelin and membrane spacing is indistinguishable between transgene expressing (type I tg) and wild-type (WT) axons, suggesting that hypermyelination is caused by additional membrane wraps. Scale bars, 1 μm (Ai and Aii); 50 nm (Aiii).

(B) CNS hypermyelination in NRG1 type I overexpressing mice. Morphometric data were obtained from 4.5-month-old mice (n = 3 per genotype) following electron microscopy of spinal cord (ventro-medial region, cervical segment 7) and corpus callosum (caudal region). (Upper panels) When g ratios were plotted as a function of axon size, randomly chosen fibers in spinal cord (left) and corpus callosum (right) were on avarage hypermyelinated (open rectangles, transgenic; closed rectangles, wild-type; $p < 0.01$). (Lower panels) The size distribution of axons in the same areas was not obviously increased by neuronal NRG1 type I overexpression (white bar, transgenic; black bar, wild-type).

(C) CNS hypermyelination in NRG1 type III overexpressing mice. Same analysis as in (B), with reduced g ratios demonstrating a significant increase of myelin volume ($p < 0.01$) in brains (left) and spinal cord (right) of *Nrg1 type III* transgenic mice.

from this unexpected result that in normal development the onset of CNS myelination is likely determined by the degree of neuronal differentiation, not by the timing of an intrinsic oligodendrocyte differentiation program.

CNS Remyelination in NRG1 Type I and III Overexpressing Mice

To test whether NRG1 would have a similar stimulating effect on CNS remyelination, we induced focal demyelination by injecting lysolecithin into the ventrolateral region of the spinal cord. Surprisingly, while axons in Nrg1 overexpressing mice were clearly hypermyelinated on the contralateral side (Figure S7A), the extent of axonal remyelination in the lesion, when quantified by electron microscopy, was no different between Nrg1 type I transgenic, Nrg1 type III transgenic, and wild-type mice (Figures S7B–S7D). This is reminiscent of experiments in which both direct infusion and systemic delivery of rhGGF-2 (NRG1 type II) do not alter remyelination (Penderis et al., 2003) in a nonimmune, gliotoxin model of demyelination. Interestingly, in lesions of Nrg1 type III tg mice, Schwann cell remyelination showed hypermyelination, in line with earlier observations in the PNS (Michailov et al., 2004).

DISCUSSION

In the PNS, the entire program of glial differentiation and myelination is controlled by NRG1 type III (Garratt et al., 2000a; Jessen and Mirsky, 2005; Nave and Salzer, 2006), and many studies have reported that oligodendrocytes respond to NRG1 in vitro and ex vivo (Calaora et al., 2001; Canoll et al., 1996; Fernandez et al., 2000; Flores et al., 2000; Sussman et al., 2005; Vartanian et al., 1997, 1999). This suggested that NRG1 may also be the growth factor responsible for regulating CNS myelination, a finding that would have important clinical implications. In multiple sclerosis, the endogenous repair of demyelinated lesions could be NRG1 dependent (ffrench-Constant et al., 2004). Moreover, schizophrenia is a complex disease that has been associated with specific *Nrg1* haplotypes (Hall et al., 2006; Stefansson et al., 2002) and independently with myelin abnormalities (Davis et al., 2003; Hakak et al., 2001). Thus, the control of subcortical myelination by NRG1 could be a missing link (Corfas et al., 2004).

The Role of Neuregulins and ErbB Receptors in Myelination

Using a set of mutant and transgenic mice, we have analyzed the function of NRG1/ErbB signaling in oligodendrocytic differentiation and myelination in vivo. We quantified the impact of altered *Nrg1* gene dosage and studied mutants with Cre-mediated *Nrg1*

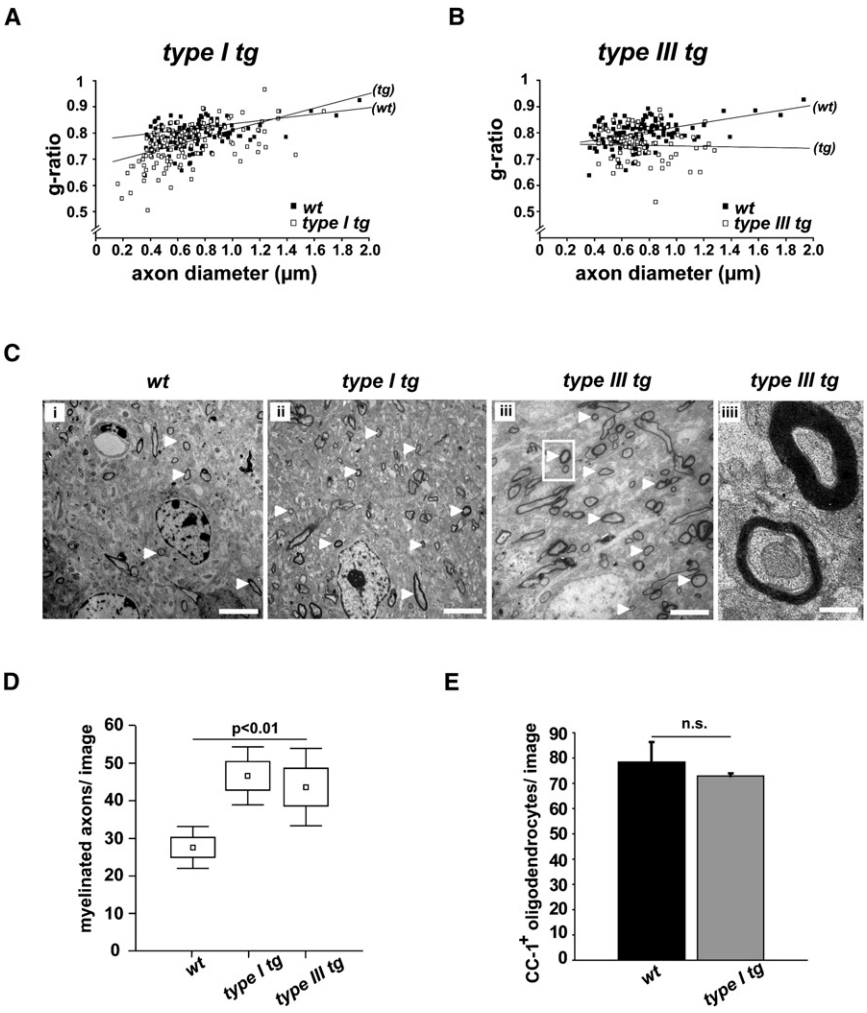

Figure 6. Transgenic Overexpression of NRG1 Type I or NRG1 Type III Stimulates Myelination in Neocortex

(A) Quantitation of cortical hypermyelination in NRG1 type I overexpressing mice. Morphometric data were obtained from 4.5-month-old animals (n = 3 per genotype) following electron microscopy of neocortical layers II/III. When g ratios were plotted as a function of axon size for randomly chosen fibers in the neocortex, hypermyelination was a feature of only the smallest (<0.4 μm) caliber axons ($p < 0.01$), leading to crossed regression lines.

(B) Cortical hypermyelination in *Nrg1 type III* transgenic mice. Same analysis as in (A), with reduced g ratios, demonstrating a significant increase of myelin volume ($p < 0.01$) in brains and spinal cord of *Nrg1 type III* transgenic mice.

(C) Electron microscopy of cortical layers II/III in 4.5-month-old mice (sagittal sections). Myelinated small-caliber axons can be recognized (some marked by white arrowheads) in wild-type mice (Ci), and more numerous in *Nrg1 type I* transgenics (Cii) and *Nrg1 type III* transgenics (Ciii). Higher magnification of boxed area (in [Ciii]) is shown on the right, depicting a normal and hypermyelinated axon (Civ). Scale bars, 10 μm (Ci–Ciii) and 500 nm (Civ).

(D) Quantification of myelin profiles (from [C]) with ten micrographs per animal analyzed (n = 3 per genotype; image size 440 μm^2). Compared to wild-type, both *NRG1 type I* and *NRG1 type III* transgenic mice have a higher number of intracortical myelinated axons in layers II/III ($p < 0.01$).

(E) Intracortical density of CC1-stained oligodendrocytes (neocortex, layer II/III) of 4.5-month-old *Nrg1 type I* transgenic mice (n = 3) is unchanged compared to wild-type controls (n = 2). Quantification (error bars, ±SD) of three images (700 μm^2) per mouse.

null mutations in cortical projection neurons, occurring either before or after oligodendrocytic specification, i.e., at E10 (Emx-Cre), E12 (NEX-Cre), or at P5 (CamKII-Cre). Contrary to our expectations, the complete absence of neuronal NRG1 did not perturb oligodendrocyte development and myelination in vivo. Even *Nestin-Cre*NRG1$^{flox/flox}$* mice exhibited normal specification of oligodendrocytes that developed on schedule (Figure 3) until early demise of these animals (the cause of death is presumably unrelated to CNS myelination).

At the receptor level, only ErbB3 and ErbB4 can bind to neuregulins (NRG1-3). ErbB1/EGFR can regulate oligodendrocyte precursor development (Aguirre et al., 2007) but fails to bind neuregulins. ErbB2 has no functional ligand-binding domain. Thus, oligodendrocytes lacking both ErbB3 and ErbB4 are incapable of transmitting signals from NRG1, NRG2, or NRG3. Most importantly, these double mutant oligodendrocytes survive and myelinate CNS axons in vivo, in marked contrast to double-mutant Schwann cells (Figure 4). This finding demonstrates that, indeed, neuregulin signaling is dispensable for CNS myelination, at least during postnatal stages.

Our results are at odds with previous reports that suggested that NRG1 is required for oligodendrocyte survival and differentiation in culture (Calaora et al., 2001; Canoll et al., 1996; Flores et al., 2000; Kim et al., 2003; Sussman et al., 2005; Vartanian et al., 1997). Specifically, the discrepancy between the present in vivo study and previous ex vivo analyses of null mutant mice is intriguing. Oligodendrocytes from *Nrg1* null or *ErbB2* null mutant mice failed to differentiate within spinal cord explants (Vartanian et al., 1999; Park et al., 2001). We have currently no explanation for these findings other than a speculative model that the electrical activity of axons may have evolved as a "myelination signal" in the CNS. Perhaps in explant cultures NRG1/ErbB signaling (i.e., the ancestral axonal myelination signal) can compensate for the absence of electrical activity in axons—but obviously not in cultures obtained from *Nrg1* or *ErbB* mutant mice.

Recently, Taveggia et al. (2008) reported cortical hypomyelination in *Nrg1 type III* heterozygous mice (Wolpowitz et al., 2000). This presents a discrepancy with our findings in the same strain of mutants (see Figures S1C and S1D) as well as in *Nrg1 null* heterozygotes (Figures S1A and S1B; all on C57BL background) and remains unexplained. Our data are supported by unaltered NRG1 protein level in the brains of heterozygote *Nrg1* (type III and null mutant) mice (Figure S1E) and the

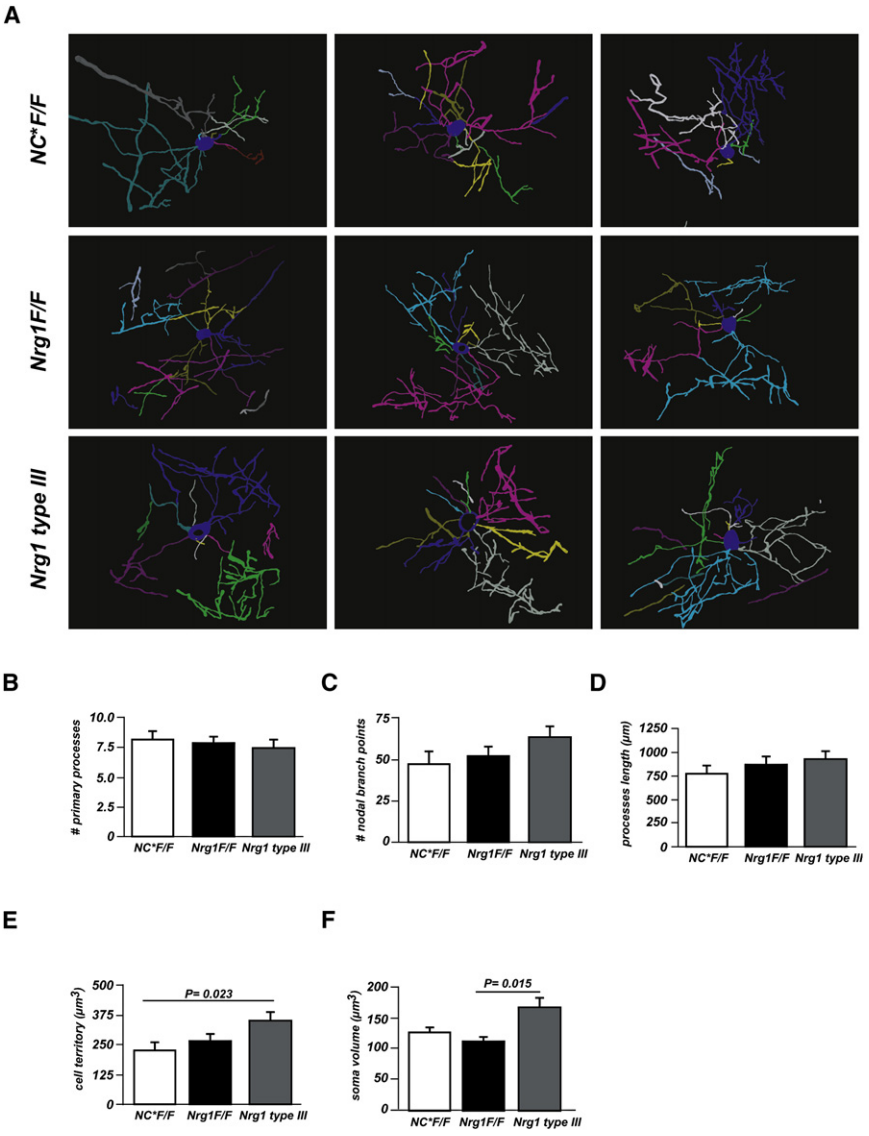

Figure 7. Oligodendrocyte Morphology

(A) Two-dimensional representations of three-dimensional tracings of CNP-stained oligodendrocytes from layers II and III of the cingulate and primary motor cortex (age 6 months). Three examples from *NEX-Cre*Nrg1*$^{flox/flox}$ mutant (NC*F/F), control (Nrg1F/F), and Nrg1 type III overexpressing mice (Nrg1 type III) are shown. Each color represents a primary cell process.

(B–F) Quantitation of primary process number (in [B]), number of nodal branch points (in [C]), avarage process length (including internodal myelin; in [D]), average 3D oligodendrocyte territory (in [E]), and average oligodendrocyte soma volume (in [F]), comparing *NEX-Cre*F/F (NC*F/F)*, *Nrg1F/F*, and *Nrg1 type III* mice (12–15 cells from three mice per genotype). Error bars, SEM. Significance test: two-tailed t test with Welch's correction or Kruskal-Wallis test.

phenotype of the various conditional null mutant mice. The effect of modifier genes in different mouse colonies could potentially explain such discrepancies.

Also, reports of CNS hypomyelination in mice overexpressing "dominant-negative" ErbB proteins under control of oligodendrocyte-specific promoters (Kim et al., 2003; Roy et al., 2007) are at variance with our findings. Unspecific side effects are the most likely explanation. For example, dominant-negative ErbB4 interacts with ErbB1/EGFR (Jones et al., 1999), a receptor regulating the development of oligodendrocyte precursor cells (Aguirre et al., 2007). Truncated ErbB receptors may also "trap" wild-type ErbB4 at specific sites in the glial-axonal junction (since mutant heterodimers will not endocytose at the normal rate). Truncated receptor dimers may occupy PDZ-binding sites or simply displace other (not yet identified) oligodendroglial receptors, which then fail to transmit axonal signals, all of which would constitute a "dominant-negative" effect. We finally note the general susceptibility of oligodendrocytes to membrane protein overexpression (Kagawa et al., 1994; Readhead et al., 1994; Tuohy et al., 2004; Turnley et al., 1991), because the expression level of dominant-negative receptors in transgenic oligodendrocytes cannot be predicted from the chosen promoter.

Can our in vivo results be explained by functional compensation between NRG1 and the structurally related growth factor Neuregulin-2 (NRG2) (Carraway et al., 1997)? *Nrg2* null mutant mice are myelinated (Britto et al., 2004), but coexpression of NRG1 and NRG2 within the CNS is limited (Busfield et al., 1997; Longart et al., 2004) (C.L. et al., unpublished data). Moreover, transgenic overexpression of NRG2 failed to increase myelin thickness in the CNS (T.M.F., M.H.S., C.L., and K.-A.N., unpublished data). Third, NRG2 is expressed in both motoneurons (Rimer et al., 2004) and DRG neurons (Figure S6E) but obviously fails to compensate for the lack of NRG1 expression in the PNS. Another candidate for compensation is Neuregulin-3 (NRG3), a more distantly related growth factor that is widely expressed in the CNS (Zhang et al., 1997). Again, *Nrg3* null mutants are viable and normally myelinated (T.M., A.N.G., and C.B., unpublished data). All this is in agreement with normal myelination of conditional ErbB3*ErbB4 double mutant mice.

Interestingly, a mild CNS hypomyelination (in addition to peripheral dysmyelination) was reported for *Bace1* mutant mice (Hu et al., 2006). While PNS effects in these mice are likely NRG1 dependent (Willem et al., 2006), our data suggest that in the CNS other proteins must be the relevant BACE1 targets. Since timely myelination requires the electrical activity of axons, the β2 subunit of the voltage-gated sodium channel (Kim et al., 2007) is an attractive candidate for BACE1 processing.

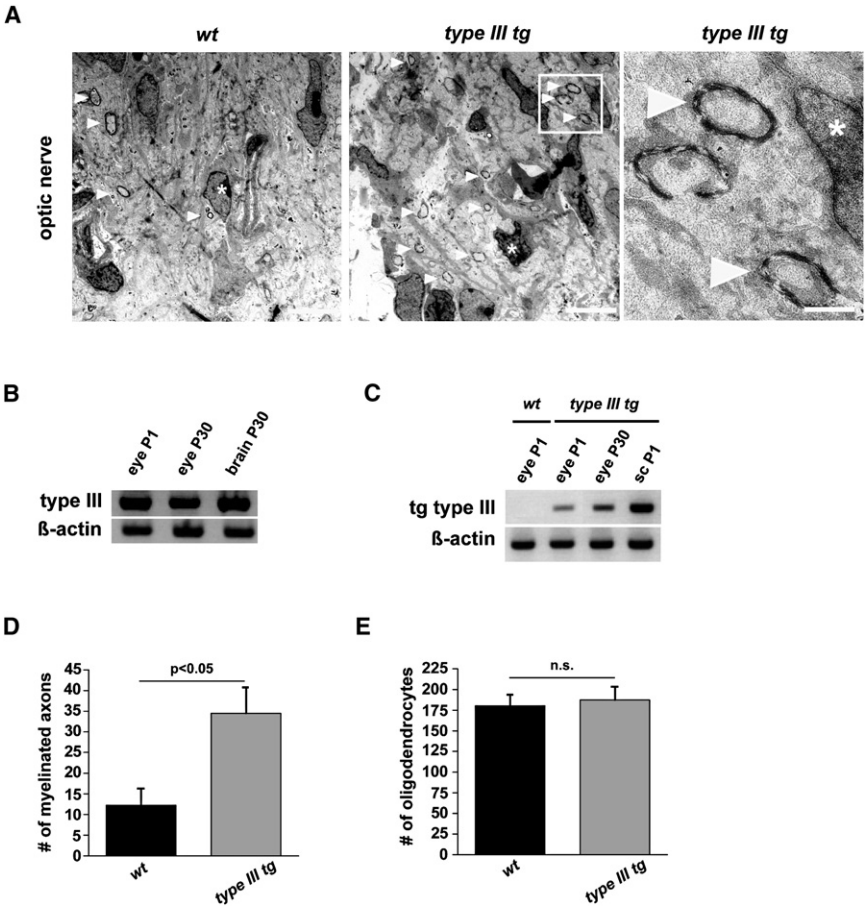

Figure 8. NRG1 Type III Stimulates Premature Myelination of the Optic Nerve

(A) Electron micrographs of developing optic nerves from wild-type (left) and *Nrg1 type III* transgenic mice (middle) at age P6, revealing single myelin profiles (arrowheads, quantified in [D]). Myelinated axons in boxed area (middle panel) are magnified on the right. Asterisks mark nuclei of oligodendrocytes. Scale bars, 5 μm.

(B) By RT-PCR, Nrg1 type III mRNA is detectable in the eye of wild-type mice at age P1 and P30 (brain mRNA serving as internal positive controls; β-actin internal control).

(C) By transgene-specific RT-PCR, type III mRNA is detectable in the eyes of postnatal (P1 and P30) *Nrg1 type III* transgenic mice, but not in wild-type (WT). Spinal cord mRNA (sc, age P1) as positive internal control; β-actin internal control.

(D and E) Higher number of myelinated axonal profiles (in [D]; $p < 0.05$) but equal number of oligodendrocytes (in [E]) in the optic nerve of 6-day-old *Nrg1 type III* transgenic mice (gray bars) when compared to age-matched controls (black bars). Quantification is from semithin cross-sections (WT, n = 5; *Nrg1 type III* transgenics, n = 6). Error bars, SEM (unpaired, two-sided t test).

In contrast to our observations in loss-of-function mutants, the neuronal overexpression of NRG1 in transgenic mice stimulated myelination, with little difference between NRG1 type III and type I isoforms. Perinatal overexpression of NRG1 type III also increased the soma size of oligodendrocytes. In contrast, proliferation of oligodendrocyte precursors was unaltered. Thus, neuronal NRG1 type III (even at several-fold elevated expression levels) appears ineffective in stimulating OPC proliferation. We hypothesize that NRG1 promotes oligodendrocyte growth by activating the PI3K/TOR/S6K pathway, because a similar "uncoupling" of oligodendrocyte proliferation and differentiation is observed in conditional mutants of the *Pten* gene (S.G. and K.-A.N., unpublished data).

That overexpression of NRG1 in retinal ganglion cells causes even premature myelination of the optic nerve is remarkable. It addresses the question whether myelination is developmentally controlled by neuronal/axonal or oligodendroglial differentiation. Our experiments reveal that manipulating neuronal differentiation is sufficient to trigger premature myelination, implying that oligodendrocytes are already myelination competent and thus "waiting" for axonal signals. The remyelination experiments further reveal that oligodendrocytes lose this responsiveness to NRG1 at an older age. This is in marked difference to Schwann cells that occasionally invade the same CNS lesion where they clearly hypermyelinate the NRG1 type III overexpressing axons (data not shown).

Possible Roles of NRG1/ErbB Signaling in Oligodendrocytes

If not required for myelination, are other oligodendroglial functions regulated by neuregulins in the CNS? Oligodendrocytes and NG2+ precursor cells are known to express NMDA, AMPA, and kainate receptors, similar to neurons and astrocytes, which coexpress ErbB4 with these glutamate receptors (Wong, 2006; Verkhratsky and Kirchhoff, 2007). Since NRG1/ErbB signaling has been implicated in the subcellular targeting and endocytosis of synaptic glutamate receptors (Gu et al., 2005; Kwon et al., 2005), it may serve a similar function for glutamate receptors on oligodendrocytes.

NRG1 may also have more subtle functions in the plasticity of cortical myelination. This relates to our observation of a 2-fold higher density of myelinated axons within the neocortex of Nrg1-transgenic mice (a number unmatched by an increase of oligodendrocyte density). Does NRG1 stimulate the generation of myelinating glial processes? Cultured neurons and oligodendrocytes reportedly increase the number of processes when NRG1 is added to the medium (Canoll et al., 1996, 1999). However, by three-dimensional cell tracing, cortical oligodendrocytes revealed about the same number of primary and secondary branches (per cell), independent of the axonal NRG1 expression level. Thus, the increased "myelin-to-oligodendrocyte" ratio is more likely caused by slightly longer internodes (which are virtually impossible to quantify in the cortex).

In conclusion, our data suggest that CNS evolution has made vertebrate oligodendrocytes independent from NRG1, presumably the ancestral signal on axons that is necessary and sufficient for myelination by Schwann cells. Perhaps, a simple system (represented by NRG1 type III/ErbB signaling to Schwann

cells) has been superseded in the CNS by a complex system that includes neuronal activity as a myelination signal. Recently identified signaling components that serve different roles in CNS and PNS myelination include purinergic receptors and activity-dependent release of ATP (Fields and Burnstock, 2006; Stevens et al., 2002). That CNS and PNS employ distinct mechanisms of glial specification and myelination control is consistent with distinct responses of oligodendrocytes and Schwann cells to neurotrophins (Chan et al., 2004).

Relevance to Neuropsychiatric Disease

With respect to human disease, *Nrg1* is an attractive susceptibility gene for schizophrenia (Stefansson et al., 2002), because this factor has been implicated in neuronal migration, synaptic plasticity, and myelination, all processes independently associated with schizophrenia (Bartzokis, 2002; Corfas et al., 2004). In particular, cortical white matter abnormalities have been repeatedly reported in SZ patients, which includes the reduced expression of myelin-related genes (Hakak et al., 2001; Tkachev et al., 2003) and decreased fractional anisotropy of callosal fibers by diffusion tensor imaging (reviewed in Dwork et al., 2007). While altered NRG1 expression levels could be a plausible cause and "missing link" to epidemiological data, our observation in mutant mice suggests otherwise. Even conditional *Nrg1* null mutants revealed quantitatively normal expression levels of structural myelin proteins (by western blotting or qRT-PCR) and also the CNS myelin ultrastructure was unaltered. Although it is difficult to make predictions across species, these data suggest that small alterations of NRG1 expression, as predicted for the *Nrg1 at risk* haplotype in humans, is highly unlikely to explain the white matter abnormalities independently documented in schizophrenia patients (Davis et al., 2003). However, several of the mouse mutants described here will be useful to study other schizophrenia-relevant functions in vivo, such as the role of the *Nrg1* gene in synaptic plasticity and cognitive functions.

EXPERIMENTAL PROCEDURES

Transgenic and Mutant Mice

The generation and genotyping of mice with *null* alleles of *Nrg1* (Meyer et al., 1997), *ErbB3* (Riethmacher et al., 1997), and *ErbB4* (Tidcombe et al., 2003), conditional *null* alleles of *Nrg1* (Li et al., 2002), *ErbB3* (T.M. and C.B. unpublished), and *ErbB4* (Golub et al., 2004), and Nrg1 type I and type III transgenes (Michailov et al., 2004) have been described. Floxed alleles of *Nrg1* are genetically *null* for alpha-NRG1 isoforms, but based on normal g ratios in comparison to wild-type and *Nrg1 null* heterozygotes (data not shown), they can be considered controls.

Cre driver lines Nestin-Cre (Tronche et al., 1999), Emx1-Cre (Gorski et al., 2002), NEX-Cre (Goebbels et al., 2006), CamKII alpha-Cre (Minichiello et al., 1999), and CNP-Cre (Lappe-Siefke et al., 2003), and Cre reporter lines R26R-lacZ (Soriano, 1999) and floxtauGFP-lacZ (Hippenmeyer et al., 2005) were also genotyped as described. For PCR, we isolated genomic DNA from tail biopsies, using Invisorb Spin tissue Mini Kit (Invitek), according to the manufacturer's directions. For routine genotyping, we used PCR primers in a coamplification reaction. Primer sequences are available upon request. All animal experiments were carried out in compliance with approved animal policies of the Max Planck Institute of Experimental Medicine.

RNA Analysis

Total RNA was extracted using Qiazol Reagent according to the manufacturer's instructions (QIAGEN). The integrity of purified RNA was confirmed using the Agilent 2100 Bioanalyser (Agilent Technologies). For RT-PCR analysis, cDNA was synthesized from total RNA using random nonamer primers and Superscript III RNase H reverse transcriptase (Invitrogen). Quantitative real-time PCR was carried out using the ABI Prism 7700 Sequence Detection System and SYBR Green Master Mix according to the manufacturer's instructions (Applied Biosystems). Reactions were carried out at least in triplicate. The relative quantity (RQ) of RNA was calculated using 7500 Fast System SDS software Ver 1.3 (Applied Biosystems). Results were depicted as histograms (generated by Microsoft Excel 2003) of normalized RQ values, with maximum RQ value in a given group normalized to 100%. PCR primer sequences are available upon request.

Protein Analysis

Protein lysates were prepared using an Ultraturrax (T8). Tissues were homogenized in 1 ml of modified RIPA buffer and protease inhibitors (Complete tablets, Roche). For western blotting, 50 μg (for NRG1) or 1–5 μg (for myelin proteins) of cortical or total brain lysate was size-separated on 8%–10% (NRG1) or 12% (myelin proteins) SDS-polyacrylamide gels and blotted onto PVDF membranes (Hybond-P) following instructions from Invitrogen. Membranes were incubated with primary antibodies as described in Supplemental Data. The densitometeric analysis of scanned ECL films was carried out using QuantityOne and ImageJ software from BioRad.

Histology and Immunostaining

Mice (P7 and older) were anesthetized with avertin and perfused with 4% paraformaldehyde in 0.1 M PBS. Brains, spinal cords, and sciatic nerves were post-fixed in 4% paraformaldehyde for 1 hr to overnight at 4°C and embedded in paraplast. Microtome sections (5–7 μm) were haematoxylin-eosin (H&E) or Nissl stained for studying brain cytoarchitecture. Myelinated fibers were visualized by Gallyas silver staining. Axonal architecture of the neocortex was studied by Bielschowsky silver impregnation. For immunofluorescent staining, paraffin sections were incubated overnight with primary antibodies against CNP (mM; 1:150, Sigma), GFAP (pRb; 1:200, DAKO), MBP (pRb; 1:500; DAKO), CC-1 (mM; 1:50; Calbiochem), NeuN (mM; 1:100, Chemicon), Olig2 (pRb; 1:20,000, a gift of C. Stiles), FNP7 (mM; 1:150, Zytomed Systems), Krox20 (pRb; 1:400, a gift of D. Meijer), NRG1 (pRb; 1:100, Santa Cruz Biotech), and MPZ (mM; 1:1000, a gift from J.J. Archelos). Sections were further incubated with their corresponding secondary Cy2 (1:100, Jackson ImmunoResearch) or Cy3 (1:1000, Jackson ImmunoResearch) antibody for 1 hr at room temperature. For DAB-based immunostaining, the Dako-LSAB$_2$ kit was used according to the manufacturer's instructions. Digital images of stained sections were obtained using Axiophot (Zeiss, Germany) and DMRXA (Leica, Germany) microscopes and Openlab 3.1.1 software (Improvision). All images were processed with Photoshop CS and Illustrator 10 software (Adobe).

Imaging Oligodendrocyte Morphology

Sections were immunostained as described in Supplemental Data. A Zeiss laser-scanning confocal microscope (Meta 510) was used to acquire z stacks of OLs at optical slices of 0.53 μm with a 63× objective (1.4 numerical aperture). Confocal z stacks were used to trace 12 to 15 individual OLs per genotype (from n = 3 mice each) with the AutoNeuron software package from the Neurolucida three-dimensional cell tracing system (MBF Biosciences, Williston, VT). Cell tracings were analyzed with the Neuroexplorer software (MBF Biosciences, Williston, VT). Statistical Data analysis (two-tailed t test with Welch's correction and one-way ANOVA test or Kruskal-Wallis test) was performed using the GraphPad Prism software package.

Electron Microscopy and Morphometry

Mice were perfused with 4% paraformaldehyde and 2.5% glutaraldehyde in 0.1 M PBS. Spinal cord, cortex, corpus callosum, optic nerves, and sciatic nerves were removed, contrasted with osmium tetroxide, and Epon embedded. Semithin sections (0.5 μm) were cut using a microtome (Leica, RM 2155) with a diamond knife (Histo HI 4317, Diatome). Sections were stained with azur II-methylenblue for 1 min at 60°C. Light microscopic observation was with a 100× lens (Leica DMRXA), and images were digitalized and analyzed with Openlab 3.1.1 and Scian Image software. For electron microscopy

of cortex, corpus callosum, optic nerve, and sciatic nerve, ultrathin (50–70 nm) sections were stained with 1% uranylacetate solution and analyzed using a Zeiss EM10 or EM109 (Leo). The g ratio was determined by dividing the circumference of an axon (without myelin) by the circumference of the same axon including myelin. At least 100 fibers per animal were analyzed, using three to six animals per genotype. Statistical analyses were performed using Statistica 6.0 (StatSoft, Tulsa, USA).

SUPPLEMENTAL DATA

The Supplemental Data include figures and Supplemental Experimental Procedures and can be found with this article online at http://www.neuron.org/cgi/content/full/59/4/581/DC1/.

ACKNOWLEDGMENTS

We thank A. Fahrenholz and P. Soban for help with histology; G. Fricke-Bode for cell culture work; W. Möbius, T. Ruhwedel, and C. Griffel for help with electron microscopy; and I. Bormuth for brain sections of NEXCre*floxtau-GFP-lacZ mice. We thank S. Emme, M. Schindler, and S. Thiel (MPI, Göttingen) for generating transgenic mice; E. Rhode (MDC Berlin) for help with ES cell culture; P. Stallerow and C. Päseler (MDC Berlin) for help with animal husbandry; and B. Jerchow and K. Becker for blastocyst injections. We also thank M. Gassman for providing ErbB4 mutants; R. Klein for *CamKII-Cre* mice; G. Schütz for *Nestin-Cre* mice; K. Jones for *Emx-Cre* mice; and S. Arber for floxtau-GFP-lacZ mice. We acknowledge C. Stiles for Olig2 antibody; M. Less for PLP antibody 3F4; D. Meijer for Krox20 antibody; J.J. Archelos for MPZ antibody; and J. Salzer, M. Simons, and members of the Nave lab for helpful discussions. K.-A.N. acknowledges grant support from the Deutsche Forschungsgemeinschaft (CMPB), the National Multiple Sclerosis Society, the Hertie Institute of MS Research, the Myelin Project, and the BMBF. C.B., T.M., A.N.G., and H.W. are supported by grants from the Deutsche Forschungsgemeinschaft (SFB 665) and the BMBF. C.L. is supported by the National Institutes of Health (NS32367). We dedicate this paper to the memory of C.H., who tragically died.

B.G.B. generated and analyzed Nrg1 type I and III transgenic mice and performed electron microscopy and morphometry; A.A. generated CaMKII-Cre*Nrg1$^{flox/flox}$, Emx1Cre*Nrg1$^{flox/flox}$, NEXCre*Nrg1$^{flox/flox}$, and Nestin-Cre*Nrg1$^{flox/flox}$ mice and analyzed them biochemically, histologically, and morphometrically; M.W.S. supervised B.G.B. and contributed to the manuscript; A.N.G. analyzed NEXCre*Nrg1$^{flox/flox}$ and cardiac-rescued *ErbB4*$^{-/-}$ mice; T.M. and H.W. generated and analyzed CNPCre*ErbB3$^{flox/-}$; ErbB4$^{flox/flox}$ mice. R.M.S., supervised by R.J.F., perfomed remyelination experiments. S.N. performed in vitro myelination experiments; C.H. and V.V. analyzed Nrg1 transgenic mice; S.G. generated NEX-Cre mice; T.M.F. and C.L. generated NRG1 expression constructs and Nrg2 transgenic mice; K.R. and H.E. analyzed mouse behavior; C.B. provided floxed and heterozygous Nrg1 mice; M.H.S. planned experiments, supervised C.H. and V.V., and contributed to the manuscript; K.-A.N. designed the study, supervised A.A. and S.N., and wrote the manuscript.

Accepted: June 27, 2008
Published: August 27, 2008

REFERENCES

Adlkofer, K., and Lai, C. (2000). Role of neuregulins in glial cell development. Glia *29*, 104–111.

Aguirre, A., Dupree, J.L., Mangin, J.M., and Gallo, V. (2007). A functional role for EGFR signaling in myelination and remyelination. Nat. Neurosci. *10*, 990–1002.

Bartzokis, G. (2002). Schizophrenia: breakdown in the well-regulated lifelong process of brain development and maturation. Neuropsychopharmacology *27*, 672–683.

Britto, J.M., Lukehurst, S., Weller, R., Fraser, C., Qiu, Y., Hertzog, P., and Busfield, S.J. (2004). Generation and characterization of neuregulin-2-deficient mice. Mol. Cell. Biol. *24*, 8221–8226.

Busfield, S.J., Michnick, D.A., Chickering, T.W., Revett, T.L., Ma, J., Woolf, E.A., Comrack, C.A., Dussault, B.J., Woolf, J., Goodearl, A.D., and Gearing, D.P. (1997). Characterization of a neuregulin-related gene, Don-1, that is highly expressed in restricted regions of the cerebellum and hippocampus. Mol. Cell. Biol. *17*, 4007–4014.

Calaora, V., Rogister, B., Bismuth, K., Murray, K., Brandt, H., Leprince, P., Marchionni, M., and Dubois-Dalcq, M. (2001). Neuregulin signaling regulates neural precursor growth and the generation of oligodendrocytes in vitro. J. Neurosci. *21*, 4740–4751.

Canoll, P.D., Kraemer, R., Teng, K.K., Marchionni, M.A., and Salzer, J.L. (1999). GGF/neuregulin induces a phenotypic reversion of oligodendrocytes. Mol. Cell. Neurosci. *13*, 79–94.

Canoll, P.D., Musacchio, J.M., Hardy, R., Reynolds, R., Marchionni, M.A., and Salzer, J.L. (1996). GGF/neuregulin is a neuronal signal that promotes the proliferation and survival and inhibits the differentiation of oligodendrocyte progenitors. Neuron *17*, 229–243.

Carraway, K.L., 3rd, Weber, J.L., Unger, M.J., Ledesma, J., Yu, N., Gassmann, M., and Lai, C. (1997). Neuregulin-2, a new ligand of ErbB3/ErbB4-receptor tyrosine kinases. Nature *387*, 512–516.

Chan, J.R., Watkins, T.A., Cosgaya, J.M., Zhang, C., Chen, L., Reichardt, L.F., Shooter, E.M., and Barres, B.A. (2004). NGF controls axonal receptivity to myelination by Schwann cells or oligodendrocytes. Neuron *43*, 183–191.

Colello, R.J., and Pott, U. (1997). Signals that initiate myelination in the developing mammalian nervous system. Mol. Neurobiol. *15*, 83–100.

Corfas, G., Roy, K., and Buxbaum, J.D. (2004). Neuregulin 1-erbB signaling and the molecular/cellular basis of schizophrenia. Nat. Neurosci. *7*, 575–580.

Davis, K.L., Stewart, D.G., Friedman, J.I., Buchsbaum, M., Harvey, P.D., Hof, P.R., Buxbaum, J., and Haroutunian, V. (2003). White matter changes in schizophrenia: evidence for myelin-related dysfunction. Arch. Gen. Psychiatry *60*, 443–456.

Duncan, I.D., and Hoffman, R.L. (1997). Schwann cell invasion of the central nervous system of the myelin mutants. J. Anat. *190*, 35–49.

Dwork, A.J., Mancevski, B., and Rosoklija, G. (2007). White matter and cognitive function in schizophrenia. Int. J. Neuropsychopharmacol. *10*, 513–536.

Esper, R.M., Pankonin, M.S., and Loeb, J.A. (2006). Neuregulins: versatile growth and differentiation factors in nervous system development and human disease. Brain Res. Brain Res. Rev. *51*, 161–175.

Falls, D.L. (2003). Neuregulins: functions, forms, and signaling strategies. Exp. Cell Res. *284*, 14–30.

Fernandez, P.A., Tang, D.G., Cheng, L., Prochiantz, A., Mudge, A.W., and Raff, M.C. (2000). Evidence that axon-derived neuregulin promotes oligodendrocyte survival in the developing rat optic nerve. Neuron *28*, 81–90.

ffrench-Constant, C., Colognato, H., and Franklin, R.J. (2004). Neuroscience. The mysteries of myelin unwrapped. Science *304*, 688–689.

Fields, R.D., and Burnstock, G. (2006). Purinergic signalling in neuron-glia interactions. Nat. Rev. Neurosci. *7*, 423–436.

Flames, N., Long, J.E., Garratt, A.N., Fischer, T.M., Gassmann, M., Birchmeier, C., Lai, C., Rubenstein, J.L., and Marin, O. (2004). Short- and long-range attraction of cortical GABAergic interneurons by neuregulin-1. Neuron *44*, 251–261.

Flores, A.I., Mallon, B.S., Matsui, T., Ogawa, W., Rosenzweig, A., Okamoto, T., and Macklin, W.B. (2000). Akt-mediated survival of oligodendrocytes induced by neuregulins. J. Neurosci. *20*, 7622–7630.

Garratt, A.N., Britsch, S., and Birchmeier, C. (2000a). Neuregulin, a factor with many functions in the life of a schwann cell. Bioessays *22*, 987–996.

Garratt, A.N., Voiculescu, O., Topilko, P., Charnay, P., and Birchmeier, C. (2000b). A dual role of erbB2 in myelination and in expansion of the schwann cell precursor pool. J. Cell Biol. *148*, 1035–1046.

Goebbels, S., Bormuth, I., Bode, U., Hermanson, O., Schwab, M.H., and Nave, K.A. (2006). Genetic targeting of principal neurons in neocortex and hippocampus of NEX-Cre mice. Genesis *44*, 611–621.

Golub, M.S., Germann, S.L., and Lloyd, K.C. (2004). Behavioral characteristics of a nervous system-specific erbB4 knock-out mouse. Behav. Brain Res. *153*, 159–170.

Gorski, J.A., Talley, T., Qiu, M., Puelles, L., Rubenstein, J.L., and Jones, K.R. (2002). Cortical excitatory neurons and glia, but not GABAergic neurons, are produced in the Emx1-expressing lineage. J. Neurosci. *22*, 6309–6314.

Gu, Z., Jiang, Q., Fu, A.K., Ip, N.Y., and Yan, Z. (2005). Regulation of NMDA receptors by neuregulin signaling in prefrontal cortex. J. Neurosci. *25*, 4974–4984.

Hakak, Y., Walker, J.R., Li, C., Wong, W.H., Davis, K.L., Buxbaum, J.D., Haroutunian, V., and Fienberg, A.A. (2001). Genome-wide expression analysis reveals dysregulation of myelination-related genes in chronic schizophrenia. Proc. Natl. Acad. Sci. USA *98*, 4746–4751.

Hall, J., Whalley, H.C., Job, D.E., Baig, B.J., McIntosh, A.M., Evans, K.L., Thomson, P.A., Porteous, D.J., Cunningham-Owens, D.G., Johnstone, E.C., and Lawrie, S.M. (2006). A neuregulin 1 variant associated with abnormal cortical function and psychotic symptoms. Nat. Neurosci. *9*, 1477–1478.

Hippenmeyer, S., Vrieseling, E., Sigrist, M., Portmann, T., Laengle, C., Ladle, D.R., and Arber, S. (2005). A developmental switch in the response of DRG neurons to ETS transcription factor signaling. PLoS Biol. *3*, e159.

Hu, X., Hicks, C.W., He, W., Wong, P., Macklin, W.B., Trapp, B.D., and Yan, R. (2006). Bace1 modulates myelination in the central and peripheral nervous system. Nat. Neurosci. *9*, 1520–1525.

Jessen, K.R., and Mirsky, R. (2005). The origin and development of glial cells in peripheral nerves. Nat. Rev. Neurosci. *6*, 671–682.

Jones, F.E., Welte, T., Fu, X.Y., and Stern, D.F. (1999). ErbB4 signaling in the mammary gland is required for lobuloalveolar development and Stat5 activation during lactation. J. Cell Biol. *147*, 77–88.

Kagawa, T., Ikenaka, K., Inoue, Y., Kuriyama, S., Tsujii, T., Nakao, J., Nakajima, K., Aruga, J., Okano, H., and Mikoshiba, K. (1994). Glial cell degeneration and hypomyelination caused by overexpression of myelin proteolipid protein gene. Neuron *13*, 427–442.

Kim, J.Y., Sun, Q., Oglesbee, M., and Yoon, S.O. (2003). The role of ErbB2 signaling in the onset of terminal differentiation of oligodendrocytes in vivo. J. Neurosci. *23*, 5561–5571.

Kim, D.Y., Carey, B.W., Wang, H., Ingano, L.A., Binshtok, A.M., Wertz, M.H., Pettingell, W.H., He, P., Lee, V.M., Woolf, C.J., and Kovacs, D.M. (2007). BACE1 regulates voltage-gated sodium channels and neuronal activity. Nat. Cell Biol. *9*, 755–764.

Kwon, O.B., Longart, M., Vullhorst, D., Hoffman, D.A., and Buonanno, A. (2005). Neuregulin-1 reverses long-term potentiation at CA1 hippocampal synapses. J. Neurosci. *25*, 9378–9383.

Lappe-Siefke, C., Goebbels, S., Gravel, M., Nicksch, E., Lee, J., Braun, P.E., Griffiths, I.R., and Nave, K.A. (2003). Disruption of Cnp1 uncouples oligodendroglial functions in axonal support and myelination. Nat. Genet. *33*, 366–374.

Law, A.J., Lipska, B.K., Weickert, C.S., Hyde, T.M., Straub, R.E., Hashimoto, R., Harrison, P.J., Kleinman, J.E., and Weinberger, D.R. (2006). Neuregulin 1 transcripts are differentially expressed in schizophrenia and regulated by 5′ SNPs associated with the disease. Proc. Natl. Acad. Sci. USA *103*, 6747–6752.

Li, L., Cleary, S., Mandarano, M.A., Long, W., Birchmeier, C., and Jones, F.E. (2002). The breast proto-oncogene, HRGalpha regulates epithelial proliferation and lobuloalveolar development in the mouse mammary gland. Oncogene *21*, 4900–4907.

Longart, M., Liu, Y., Karavanova, I., and Buonanno, A. (2004). Neuregulin-2 is developmentally regulated and targeted to dendrites of central neurons. J. Comp. Neurol. *472*, 156–172.

Lopez-Bendito, G., Cautinat, A., Sanchez, J.A., Bielle, F., Flames, N., Garratt, A.N., Talmage, D.A., Role, L.W., Charnay, P., Marin, O., and Garel, S. (2006). Tangential neuronal migration controls axon guidance: a role for neuregulin-1 in thalamocortical axon navigation. Cell *125*, 127–142.

Mei, L., and Xiong, W.C. (2008). Neuregulin 1 in neural development, synaptic plasticity and schizophrenia. Nat. Rev. Neurosci. *9*, 437–452.

Meyer, D., Yamaai, T., Garratt, A., Riethmacher-Sonnenberg, E., Kane, D., Theill, L.E., and Birchmeier, C. (1997). Isoform-specific expression and function of neuregulin. Development *124*, 3575–3586.

Michailov, G.V., Sereda, M.W., Brinkmann, B.G., Fischer, T.M., Haug, B., Birchmeier, C., Role, L., Lai, C., Schwab, M.H., and Nave, K.A. (2004). Axonal neuregulin-1 regulates myelin sheath thickness. Science *304*, 700–703.

Minichiello, L., Korte, M., Wolfer, D., Kuhn, R., Unsicker, K., Cestari, V., Rossi-Arnaud, C., Lipp, H.P., Bonhoeffer, T., and Klein, R. (1999). Essential role for TrkB receptors in hippocampus-mediated learning. Neuron *24*, 401–414.

Nave, K.A., and Salzer, J.L. (2006). Axonal regulation of myelination by neuregulin 1. Curr. Opin. Neurobiol. *16*, 492–500.

Park, S.K., Miller, R., Krane, I., and Vartanian, T. (2001). The erbB2 gene is required for the development of terminally differentiated spinal cord oligodendrocytes. J. Cell Biol. *154*, 1245–1258.

Penderis, J., Woodruff, R.H., Lakatos, A., Li, W.W., Dunning, M.D., Zhao, C., Marchionni, M., and Franklin, R.J. (2003). Increasing local levels of neuregulin (glial growth factor-2) by direct infusion into areas of demyelination does not alter remyelination in the rat CNS. Eur. J. Neurosci. *18*, 2253–2264.

Readhead, C., Schneider, A., Griffiths, I., and Nave, K.A. (1994). Premature arrest of myelin formation in transgenic mice with increased proteolipid protein gene dosage. Neuron *12*, 583–595.

Riethmacher, D., Sonnenberg-Riethmacher, E., Brinkmann, V., Yamaai, T., Lewin, G.R., and Birchmeier, C. (1997). Severe neuropathies in mice with targeted mutations in the ErbB3 receptor. Nature *389*, 725–730.

Rimer, M., Prieto, A.L., Weber, J.L., Colasante, C., Ponomareva, O., Fromm, L., Schwab, M.H., Lai, C., and Burden, S.J. (2004). Neuregulin-2 is synthesized by motor neurons and terminal Schwann cells and activates acetylcholine receptor transcription in muscle cells expressing ErbB4. Mol. Cell. Neurosci. *26*, 271–281.

Roy, K., Murtie, J.C., El-Khodor, B.F., Edgar, N., Sardi, S.P., Hooks, B.M., Benoit-Marand, M., Chen, C., Moore, H., O'Donnell, P., et al. (2007). Loss of erbB signaling in oligodendrocytes alters myelin and dopaminergic function, a potential mechanism for neuropsychiatric disorders. Proc. Natl. Acad. Sci. USA *104*, 8131–8136.

Sagane, K., Hayakawa, K., Kai, J., Hirohashi, T., Takahashi, E., Miyamoto, N., Ino, M., Oki, T., Yamazaki, K., and Nagasu, T. (2005). Ataxia and peripheral nerve hypomyelination in ADAM22-deficient mice. BMC Neurosci. *6*, 33.

Schmucker, J., Ader, M., Brockschnieder, D., Brodarac, A., Bartsch, U., and Riethmacher, D. (2003). erbB3 is dispensable for oligodendrocyte development in vitro and in vivo. Glia *44*, 67–75.

Soriano, P. (1999). Generalized lacZ expression with the ROSA26 Cre reporter strain. Nat. Genet. *21*, 70–71.

Stefansson, H., Sigurdsson, E., Steinthorsdottir, V., Bjornsdottir, S., Sigmundsson, T., Ghosh, S., Brynjolfsson, J., Gunnarsdottir, S., Ivarsson, O., Chou, T.T., et al. (2002). Neuregulin 1 and susceptibility to schizophrenia. Am. J. Hum. Genet. *71*, 877–892.

Stevens, B., Porta, S., Haak, L.L., Gallo, V., and Fields, R.D. (2002). Adenosine: a neuron-glial transmitter promoting myelination in the CNS in response to action potentials. Neuron *36*, 855–868.

Sussman, C.R., Vartanian, T., and Miller, R.H. (2005). The ErbB4 neuregulin receptor mediates suppression of oligodendrocyte maturation. J. Neurosci. *25*, 5757–5762.

Taveggia, C., Zanazzi, G., Petrylak, A., Yano, H., Rosenbluth, J., Einheber, S., Xu, X., Esper, R.M., Loeb, J.A., Shrager, P., et al. (2005). Neuregulin-1 type III determines the ensheathment fate of axons. Neuron *47*, 681–694.

Taveggia, C., Thaker, P., Petrylak, A., Caporaso, G.L., Toews, A., Falls, D.L., Einheber, S., and Salzer, J.L. (2008). Type III neuregulin-1 promotes oligodendrocyte myelination. Glia *56*, 284–293.

Tidcombe, H., Jackson-Fisher, A., Mathers, K., Stern, D.F., Gassmann, M., and Golding, J.P. (2003). Neural and mammary gland defects in ErbB4

knockout mice genetically rescued from embryonic lethality. Proc. Natl. Acad. Sci. USA *100*, 8281–8286.

Tkachev, D., Mimmack, M.L., Ryan, M.M., Wayland, M., Freeman, T., Jones, P.B., Starkey, M., Webster, M.J., Yolken, R.H., and Bahn, S. (2003). Oligodendrocyte dysfunction in schizophrenia and bipolar disorder. Lancet *362*, 798–805.

Tronche, F., Kellendonk, C., Kretz, O., Gass, P., Anlag, K., Orban, P.C., Bock, R., Klein, R., and Schutz, G. (1999). Disruption of the glucocorticoid receptor gene in the nervous system results in reduced anxiety. Nat. Genet. *23*, 99–103.

Tuohy, T.M., Wallingford, N., Liu, Y., Chan, F.H., Rizvi, T., Xing, R., Bebo, B., Rao, M.S., and Sherman, L.S. (2004). CD44 overexpression by oligodendrocytes: a novel mouse model of inflammation-independent demyelination and dysmyelination. Glia *47*, 335–345.

Turnley, A.M., Morahan, G., Okano, H., Bernard, O., Mikoshiba, K., Allison, J., Bartlett, P.F., and Miller, J.F. (1991). Dysmyelination in transgenic mice resulting from expression of class I histocompatibility molecules in oligodendrocytes. Nature *353*, 566–569.

Vartanian, T., Goodearl, A., Viehover, A., and Fischbach, G. (1997). Axonal neuregulin signals cells of the oligodendrocyte lineage through activation of HER4 and Schwann cells through HER2 and HER3. J. Cell Biol. *137*, 211–220.

Vartanian, T., Fischbach, G., and Miller, R. (1999). Failure of spinal cord oligodendrocyte development in mice lacking neuregulin. Proc. Natl. Acad. Sci. USA *96*, 731–735.

Verkhratsky, A., and Kirchhoff, F. (2007). NMDA Receptors in glia. Neuroscientist *13*, 28–37.

Willem, M., Garratt, A.N., Novak, B., Citron, M., Kaufmann, S., Rittger, A., DeStrooper, B., Saftig, P., Birchmeier, C., and Haass, C. (2006). Control of peripheral nerve myelination by the beta-secretase BACE1. Science *314*, 664–666.

Wolpowitz, D., Mason, T.B., Dietrich, P., Mendelsohn, M., Talmage, D.A., and Role, L.W. (2000). Cysteine-rich domain isoforms of the neuregulin-1 gene are required for maintenance of peripheral synapses. Neuron *25*, 79–91.

Wong, R. (2006). NMDA receptors expressed in oligodendrocytes. Bioessays *28*, 460–464.

Zhang, D., Sliwkowski, M.X., Mark, M., Frantz, G., Akita, R., Sun, Y., Hillan, K., Crowley, C., Brush, J., and Godowski, P.J. (1997). Neuregulin-3 (NRG3): a novel neural tissue-enriched protein that binds and activates ErbB4. Proc. Natl. Acad. Sci. USA *94*, 9562–9567.